V. 感染症

ニューモシスチス肺炎

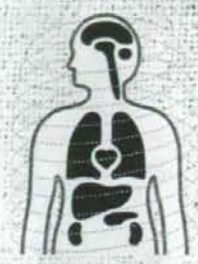

長崎大学附属病院感染制御教育センター
安岡 彰

診断に要する基礎知識

ニューモシスチス肺炎(かつてのカリニ肺炎)は，免疫不全状態で発症する致死率の高い重症肺炎である．HIV 感染症や悪性リンパ腫，免疫抑制薬・抗癌薬や，中等量以上の副腎皮質ステロイドホルモンの持続投与といった，何らかの免疫不全状態が背景にあることがほとんどであるが，これらの免疫不全が診断されないままにニューモシスチス肺炎を発症して発見される例が増加してきている．とくに最近の HIV 感染者に発症するニューモシスチス肺炎の 8 割は，これまで HIV 感染症と診断されていない「健常者」の「市中肺炎」として発見されていることから，本症の特徴的画像に類似した病態をみた場合には，鑑別にあげることが重要である．

ニューモシスチス肺炎の臨床所見として発熱，乾性咳嗽，呼吸困難があげられているが，すべてが揃うのは病態が進行してからである．胸部 X 線で，びまん性の陰影が出現してからは朝夕でも所見が変わるほど進行が早いとされているが，これは進行した状態で診断されることが多かったためで，実際は数日から数週間(HIV 感染症の場合)の亜急性の経過で，発熱や咳，息切れなどが漸次みられることが多い．

画像診断のポイントと次の一手

胸部 X 線では，びまん性でほぼ左右対称性の淡いすりガラス陰影が特徴である(Fig. 1)．肺門部に強く，外側胸壁側には淡い傾向がある．また典型例では，肺尖より下肺のほうが陰影が濃いとされている．初期では肺門部の血管影の輪郭が不鮮明という程度の所見しかない場合や，胸部 X 線では明らかな所見を指摘できない場合もある．一方進行例では，consolidation といってもよいような気管支透亮像を伴った均一な陰影となることもある．この場合も末梢側をみると，すりガラス状の部分がみられることが多い．

胸部 CT(HR-CT が望ましい)では，肺小葉単位で均一な肺野濃度の上昇が認められる(Fig. 2)．胸部 X 線でみるよりも個々の肺小葉の濃度上昇は明らかである．小葉間での程度の差がはっきりとみられる場合が多く，地図状分布と呼ばれる

<画像オーダーのポイント>

- 呼吸器症状が目立たない時期でも，不明熱診断の手順に則って胸部 X 線を撮影する．初期病変では肺門部血管影の不鮮明化程度の所見しかない場合もあるので，注目して読影する．
- 胸部 X 線で淡い陰影が疑われる場合は，胸部 CT を施行する．HR-CT が望ましい．ニューモシスチス肺炎の診断目的としては，造影 CT は必須ではない．
- 胸部 X 線や HR-CT でも所見が明らかではないが免疫不全の背景から本症が疑われる場合は，ガリウム(Ga)シンチグラムを追加する場合もある．

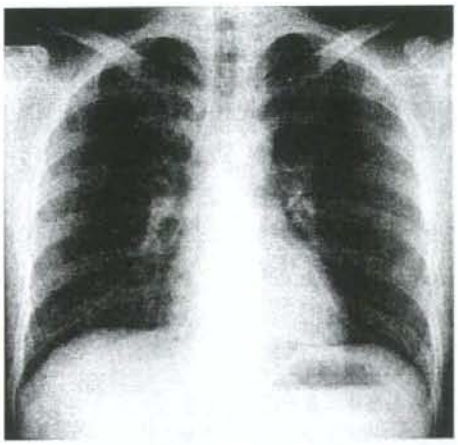

Fig. 1. 胸部 X 線
びまん性で，ほぼ左右対称の淡いすりガラス陰影が認められる．

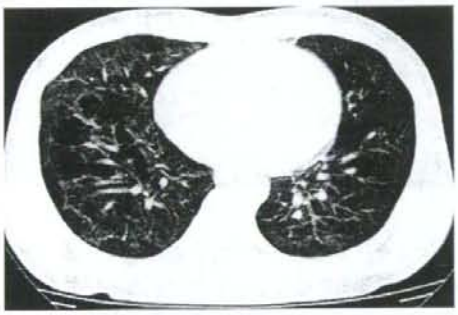

Fig. 3. 胸部 CT
地図状分布がみられる．

(Fig. 3)．胸部 X 線と同様に，胸壁側には陰影が少なく，スペアされたようにみえる (peripheral sparing)．陰影は基本的に両側，びまん性にみられることが多い．また嚢胞性変化や，下肺背側の

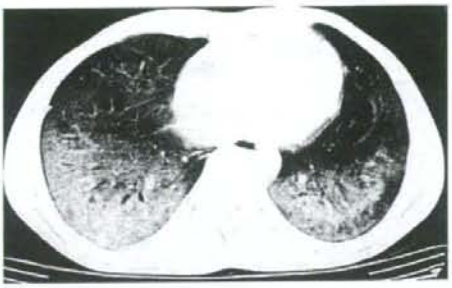

Fig. 2. 胸部 CT
肺小葉単位で均一な肺野濃度の上昇がみられる．

<注意すべき所見>
- ニューモシスチス肺炎の画像所見では，多彩な例外所見が報告されている．塊状影，結節影，多発粒状影や限局した浸潤影，多発嚢胞性陰影，胸水などの報告がある．
- このような場合も，周囲に特徴的なすりガラス状陰影がみられる場合が多いため，この所見から本症を疑うことが肝要である．

結節状の陰影がみられやすい．胸水がみられることは少ない．

胸部 X 線や CT で明らかとなる以前の早期から，Ga シンチグラムにて肺野でびまん性に取り込みの亢進がみられる．Ga シンチグラムはニューモシスチス肺炎の診断には必須ではないが，必要な場合は検査を考慮する．

画像上疑わしい場合には，LDH や β-glucan，KL-6 など，本症で上昇することが知られている血液生化学的検査を行うとともに，呼吸器検体を採取して顕微鏡的に病原体検出を試みる．本症の病原体である *Pneumocystis jirovecii* は，培養することができない．

IMAGE QUIZ

34歳，男性．HIV感染症，ニューモシスチス肺炎と診断され，3日前からST合剤で治療を開始した．突然呼吸困難を訴えたため，胸部X線を撮影した(Fig. 4)．

呼吸困難の原因を推定せよ．

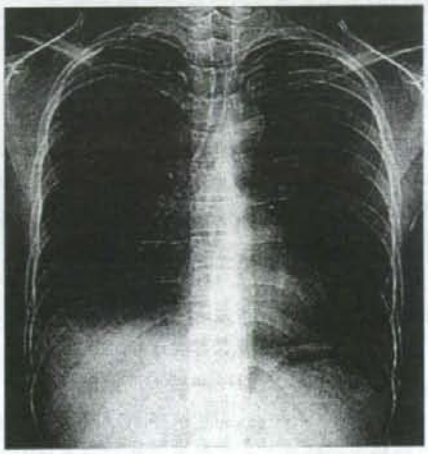

Fig. 4. 胸部X線

解説

右上肺野に胸郭と平行した方向にラインが観察され，その胸郭側には肺胞構造がみられない．気胸が認められる．

ニューモシスチス肺炎では，組織壊死やチェックバルブ機構により，肺末梢側の気腫性変化が起こりやすく，気胸を起こす頻度が高い．ニューモシスチス肺炎治療中に急に呼吸困難が増強した場合は，気胸の発生を念頭に置き，速やかに胸部X線を撮影して，慎重に読影する必要がある．

エイズにおける日和見感染症の早期発見と最適治療

長崎大学医学部・歯学部附属病院感染制御教育センター教授　安岡　彰（やすおか　あきら）

❶HIV にみられる日和見感染症の現状

日本においてはHIV感染者の増加のみならず，免疫不全が進行し日和見感染症を発症した患者，すなわちエイズ発症者も年々増加している．

HIV 感染症は効果的な抗ウイルス療法（highly active anti-retroviral therapy；HAART）の開発と普及により，もはや致死的な疾患ではなくなった．これは患者予後の改善にとどまらず，患者に対する差別意識の改善や，医療従事者の感染に対する恐怖心を低下させるのにも役立った．一方，リスクが高い行為を抑止する効果も低減した可能性が高い．現状では早期発見のための啓発も十分とはいえないため，無症状の間に自発検査で発見される患者の比率はさほど高くない．この結果，重篤な日和見感染症で医療機関を受診し，HIV 陽性/AIDS と診断される患者の数が増加していると考えられる．

このような背景から，日本では HIV にみられる日和見感染症を一般臨床医が診断し適切に治療することが，患者予後の改善に重要な役割を果たしている．日本の現状を解析し，適切な診断・治療のための情報を提供するために，厚生労働省エイズ対策研究事業「重篤な日和見感染症の早期発見と最適治療に関する研究」班が研究を進めている．

全国 HIV 拠点病院の協力を得て研究班で集積されてきたデータをみても，日和見感染症は増加の一途にあり（図 1），エイズ指標疾患の発生比率は図 2 に示すごとくである．指標疾患のいずれかを発症した患者の死亡率は年々減少しているものの，2005 年でも約 10% と高く（疾患別累計では悪性リンパ腫の 47.5% からカンジダ症の 9.1% に分布），日和見感染症を発症することは HIV 感染者にとって大きな予後悪化因子となっている．

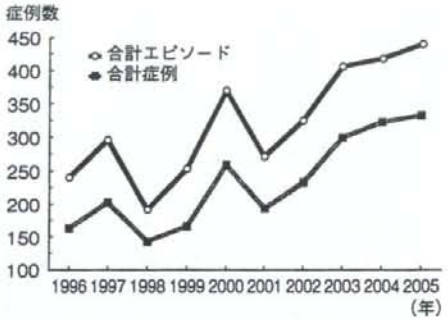

図 1　日和見感染症報告数の推移
（厚生労働科学研究エイズ対策研究事業「重篤な日和見感染症の早期発見と最適治療に関する研究」班集計）

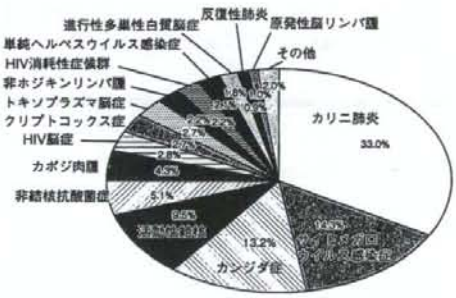

図 2　エイズ指標疾患の頻度（1995 ～ 2005 年）
（厚生労働科学研究エイズ対策研究事業「重篤な日和見感染症の早期発見と最適治療に関する研究」班集計）

❷日和見感染症の早期発見

日常診療のなかで HIV 感染症に合併した日和見感染症を発見するためには，HIV 感染症でよく認められる感染症の特徴と，HIV 感染のハイリスク要因を知り，一般的疾患とのわずかな差異を認知する必要がある．表 1 に日和見感染

表1　HIVを疑う疾患・病態

スリガラス状陰影の肺炎・間質性肺炎……ニューモシスチス肺炎
肺結核，特に肺炎様の陰影をとるもの，肺門・縦隔リンパ節腫張が目立つもの
肺の多発性粒状陰影……粟粒結核
食道の乳白色白苔付着……カンジダ食道炎，サイトメガロウイルス(CMV)食道炎
食道潰瘍……カンジダ食道炎，CMV食道炎など
節外性の悪性リンパ腫
眼底の血管に沿った浸出性出血性病変……CMV網膜炎
大腸潰瘍（潰瘍性大腸炎様）……大腸アメーバ症，CMV腸炎
暗～紫赤色のやや硬い皮膚隆起……カポジ肉腫，bacillary angiomatosis
脳内の占拠性病変……脳リンパ腫，トキソプラズマ脳症

表2　HIVを疑う背景・既往歴

性感染症
梅毒，淋病，クラミジアなどの非淋菌性尿道炎
性感染症も起こす感染症
A型肝炎，B型肝炎，赤痢アメーバ症，ジアルジア症
帯状疱疹
複数の薬剤に対する過敏症

症の特徴的所見からみたHIV感染症を鑑別すべき病態を列挙した．特に，表2のような背景を認める場合はHIV感染を疑って積極的にHIV抗体検査を行うことが望ましい．

HIV抗体検査は，必要時には保険診療で検査が認められている（間質性肺炎等後天性免疫不全症候群の疾患と鑑別が難しい疾患が認められる場合と，HIVの感染に関連しやすい性感染症が認められる場合でHIV感染症を疑わせる自他覚症状がある場合）．HIVの早期発見は医療費削減にも寄与することから，必要時には検査が行われるべきである．検査には患者の同意が必要であるが，必ずしも文書での同意が求められているわけではなく，「今の疾患から万一のことを考えて念のために検査を」というスタンスで口頭による簡潔な説明と同意を得るなど，病院でのHIV抗体検査をより拡充する必要がある．

❸日和見感染症の治療―免疫再構築症候群との関連において

免疫不全で起こった日和見感染症の治療ではHAARTを併用することは理論的には正しいものの，実際は治療の複雑化や薬剤相互作用，副作用の相乗などで困難であることが多い．このため，有効な治療法が乏しい進行性多巣性白質脳症やカポジ肉腫，悪性リンパ腫などを除き，早期からのHAART併用は行わない場合が多い．

また，高度免疫不全状態での日和見感染症には免疫再構築症候群（immune reconstitution inflammatory syndrome；IRIS）の問題が発生する．これは免疫不全状態（おおむねCD4＜100/μl）で抗HIV療法を開始すると，一旦治療して改善していた日和見感染症が悪化したり，治療開始時点では顕性化していなかった潜在的日和見感染症が急激に顕性化する現象である．この対策としては，先行する日和見感染症がある場合は十分な治療を行ってから抗HIV薬を開始すること，IRISと思われる日和見感染症の発症がみられた場合には適切な治療薬と共に副腎皮質ステロイドホルモンによる過剰な炎症のコントロールを行うことが知られている．さらに，主要な疾患に対する発症予防投薬を短期間であっても行うことにより発症率を下げることができる可能性が示唆されており，現在検討を行っている．

新規HIV感染者の急増により，これまで診療に当たったことがなかった医療者にも，突然目の前に患者としてHIV感染者がやって来ることがある時代であり，基本的な日和見感染症の診療の考え方を理解することはすべての医療者に必要な知識になってきている．

Ⅱ. 呼吸器疾患

23. ウイルス性肺炎・ニューモシスチス肺炎

Viral pneumonia・Pneumocystis pneumonia

安岡 彰
YASUOKA Akira

適応症

インフルエンザ肺炎

薬剤名	下限	←	常用量	→	上限
1)リン酸オセルタミビル oserltamivir phophate (商品名：タミフル Tamiflu)	75mg		**150mg**		
2)ザナミビル水和物 zanamivir hydrate (商品名：リレンザ Relenza)	10mg		**20mg**		
3)塩酸アマンタジン amantadine hydrochloride (商品名：シンメトレル Symmetrel)			**100mg**		

使用法

1)75mgカプセルを1日2回，5日間内服.

2)1回に2プリスター中の薬剤(1プリスターに5mg)を吸入．1日2回，5日間吸入.

3)100mgを1－2回に分割投与．A型インフルエンザにのみ有効.

主作用

1)インフルエンザウイルスのノイラミニダーゼの働きを阻害することにより，感染細胞で合成されたウイルスの成熟・分離を阻害する.

2)1)と同じ．吸入により感染局所に高濃度の薬剤を到達させることができる.

3)感染したインフルエンザウイルスが細胞内で脱殻するのを阻止することにより，ウイルスの増殖を阻害する．B型インフルエンザには無効．またA型インフルエンザウイルスにも本剤に対する耐性が広がっている.

副作用と対策

1)本剤に特徴的な副作用は下痢，腹痛，嘔気などの消化器症状である．本剤の投与により10代の青年や幼児で異常行動誘発の可能性が指摘された．これについてはその後の検討により，薬剤の影響の可能性は低いとするデータが出されている．しかし現時点では，有用性とリスクを考慮して，10代の患者に対しての本剤の投与は慎重であるべきとの指示が出されている.

2)本剤は吸入での投与により病変局所へ直接薬剤を到達させるため，全身性の副作用は少ないと考えられている．吸入により気管支けいれんを誘発することがあり，とくに気管支喘息や慢性気道感染症，低酸素血症のある患者では注意が必要である.

3)めまいやふらつき，消化器症状が主な副作用である．まれに意識障害や痙攣なども注意が必要である.

いずれの副作用についても，抗インフルエンザ薬の投与継続の必要性を再度検討し，臨床症状の改善などが見られていれば，5日間の投与を短縮

長崎大学医学部・歯学部附属病院感染制御教育センター センター長

0371-1900/08/¥50/頁/JCLS

することも考慮される.

禁　忌

1)2)本剤の成分に対して過敏症の既往歴のある場合.

3)高度の腎障害，妊婦，本剤の成分に対して過敏症の既往歴のある場合.

解　説

インフルエンザによる肺炎ではウイルス自体による肺炎と，最近の2次感染による肺炎が知られている．ここで記載したのは，インフルエンザおよびインフルエンザウイルスによる肺炎の場合の治療である．ウイルス自体による肺炎はインフルエンザ発症の早期からみられ，しばしば急速に進行するため抗ウイルス剤のみではなく，肺機能の保護を目的とした治療を組み合わせる必要がある．細菌の2次感染では有効な抗菌薬の投与を行う.

適応症

サイトメガロウイルス(CMV)肺炎

薬剤名	下限	←	常用量	→	上限
1)ガンシクロビル ganciclovir (商品名：デノシン Denosine)	5 mg/kg ×1回		**5**mg/kg ×2回		
2)バルガンシクロビル valganciclovir hydrochloride (商品名：バリキサ Valixa)	900mg		**1,800**mg		
3)ホスカルネット foscarnet sodium hydrate (商品名：ホスカビル Foscavir)	90mg/kg ×1回		**90**mg/kg ×2回 **60**mg/kg ×3回		

使用法

1)初期治療：1回5 mg/kgを1日2回，12時間ごとに1時間以上かけて，14日間点滴静注.

維持治療：1日6 mg/kgを週に5日または1日5 mg/kgを週に7日，1時間以上かけて点滴静注.

2)初期治療：1回2錠(900mg)を1日2回食後に内服.

維持療法：1回900mgを1日1回食後に内服(本剤の効能・効果に肺炎は認められていない).

3)初期治療：1回90mg/kgを2時間以上かけて1日2回，点滴静注(1回60mg/kgを1日3回投与も可).

維持治療：1日1回90～120mg/kgを2時間以上かけて点滴静注(本剤の効能・効果に肺炎は認められていない).

腎機能障害を防止するため投与は十分時間をかけ，また投与前後に輸液を行い尿量を確保する．腎機能障害がある場合は，クレアチニンクリアランスに応じて投与量を減ずる.

主作用

1)活性型のガンシクロビル-三リン酸はウイルスDNA合成に際して，本来のデオキシリボ核酸であるデオキシグアノシン-三リン酸(dGTP)と競合的に拮抗して取り込まれ，DNAの合成反応を阻害することによってウイルス増殖を阻止する．ガンシクロビルから活性型のガンシクロビル-三リン酸への転換は，サイトメガロウイルス感染細胞内でのみ行われるため，人細胞のDNA合成に対する影響が少ない.

2)本剤はガンシクロビルのプロドラッグであり，腸管で吸収された後，ガンシクロビルに変換される.

3)サイトメガロウイルスのDNAポリメラーゼに直接作用してDNA合成を阻害することによりサイトメガロウイルスの増殖を抑制する．本剤は投与体が活性体である.

副作用と対策

1)2)本剤は人細胞でのDNA合成阻害が皆無ではないため，骨髄障害が高頻度に見られる．汎血球減少，重篤な白血球減少，重篤な血小板減少には最大限注意を払う必要がある．また腎障害や膵炎も認められる．このような重篤な障害を早期に発見するため，本剤投与中は週2～3回以上血液検査を行い，副作用の早期発見に努める．骨髄障害が認められた場合はすみやかに投与を中止し，G-CSFの投薬を含めた対処を行う.

3)本剤の最も重要な副作用は腎機能障害である．本剤投与にあたっては時間をかけて投与するとともに前後に輸液を行い，尿量を確保する必要がある．また，投与前および投与中に腎機能の低下が見られた場合は，添付文書に示された補正表にしたがって投与量を減ずる．そのほかの副作用として消化器症状(嘔気，嘔吐)，電解質異常(Mg，K，Caの低下)，また投与速度が早いと血圧低下やショック様症状を呈することがある．

禁　忌

1)好中球数500/mm³未満，または血小板数25,000/mm³未満の患者，妊婦または妊娠している可能性がある女性，本剤に対する過敏症の既往歴のある患者．

2)好中球数500/mm³未満，血小板数25,000/mm³未満またはヘモグロビン濃度8g/dL未満の患者，妊婦または妊娠している可能性がある女性，本剤に対する過敏症の既往歴のある患者．

3)クレアチニンクリアランス値が0.4mL/分/kg未満の患者，ニューモシスチス肺炎の治療薬であるペンタミジンを投与中の患者，本剤に対し過敏症の既往歴のある患者．

解　説

サイトメガロウイルス治療薬はいずれもDNA合成阻害によってウイルスの増殖を阻害する．ガンシクロビルおよびバルガンシクロビルは，骨髄障害，ホスカルネットは腎機能障害の副作用がほぼ必発であり，投与に際しては投与開始前の評価および投与中のモニターが重要である．

投与の選択は，投与前の骨髄抑制の有無と腎機能の程度が最大の判断要素であるが，効果発現の早さではガンシクロビルが勝っており，投与に際して制限がなければガンシクロビルを第1選択とする．軽症でない限り静注で投与開始し，治療効果が得られた時点で，バルガンシクロビルへのスイッチも考慮できる．いずれの薬剤を選択した場合も週2回以上の血液検査を施行し，副作用出現を早期に検知することが重要である．

治療は14日以上が原則で，治療効果を見ながら初期治療から引き続き維持治療へと移行する．

HIV感染症で抗HIV療法により免疫能の改善が見られた場合や，白血球減少などの発症要因が改善した場合は治療中止も可能である．造血幹細胞移植後のサイトメガロウイルス感染症では，ガンマグロブリンの併用を考慮する．

適　応　症

ニューモシスチス肺炎

薬　剤　名	下限	←	常用量	→	上限
1)ST合剤　sulfamethoxazole-trimethoprim (商品名：バクタ　Baktar， バクトラミン　Bactramin ほか)	1錠 (スルファメトキサゾール400mg，トリメトプリム80mg)		**15**mg/kg		20mg/kg
2)ペンタミジン　pentamidine isetionate (商品名：ペナンバックス Benanbax)	3 mg/kg		**4**mg/kg		
3)ジアフェニルスルホン(ダプソン) diaphenylsulfone (商品名：レクチゾール　Lectisol)			**100**mg/kg		

使　用　法

1)初期治療：トリメトプリムとして1日量15～20mg/kgを3回に分け投与．経口，点滴静注とも投与量は同じ．体重60kgで1回4錠(4アンプル)を1日3回投与となる．点滴静注では1アンプルあたり125ml(最低でも75ml)の5%ブドウ糖液を用いて溶解し，すみやかに投与を開始する．

維持治療(再発予防)：ST合剤1日1－2錠を1日1回投与する．2錠週3回とすることも可．

2)初期治療：点滴投与1日1回3～4 mg/kgを2～3時間かけて点滴静注(溶解時は注射用水3－5mLに溶解後，ブドウ糖注射液または生理食塩液250mLに希釈する)．本剤は筋注投与も用法として記載されているが，注射局所の無菌性壊

死を起こすので原則行わない.

維持治療：吸入投与，1ヵ月に1回，300mgを蒸留水に溶解し，30分程度の吸入時間となるように希釈量を調整して吸入投与．この吸入投与は軽症の初期治療としても用いることができる．この場合は1日1回吸入する.

3)初期治療には用いられない．1)，2)が使用できない場合に維持治療(発症予防)に用いられることがある.

主作用

1)合剤のいずれの薬剤も葉酸代謝経路の阻害剤で，ニューモシスチスの葉酸合成を阻害することで活性を発揮する.

2)ニューモシスチスのグルコース代謝および蛋白質合成を抑制するとされるが，正確な作用機序は明らかでない.

副作用と対策

1)本剤の重要な副作用としてはアレルギー反応で，とくにHIV感染者では頻度が高い．投与開始直後のStevens-Johnson症候群や中毒性表皮壊死症(TEN)，投与開始後5～14日頃に見られる発熱，発疹などに注意を払い，発症した場合にはすみやかに中止する．また，骨髄障害も頻度が高く白血球減少，貧血などがみられる．電解質異常(高K血症，低Na血症)も頻度が高い．本剤による腎機能障害も見られる.

2)重要な副作用は腎機能障害，膵炎，低血糖，があげられる．また投与速度が速いと低血圧やショック様症状を呈するため．添付文書に示される時間よりは長い時間をかけて(2－3時間)投与する方が安全である．このほか電解質異常や味覚異常，口唇や四肢の知覚異常の頻度も高い．本剤投与による意識障害や錯乱，骨髄障害を見ることもある．副作用を早期に発見するために本剤投与中は週2回以上の血液検査を行うとともに，自覚症状の出現に注意を払う必要がある.

3)過敏症症状，骨髄障害が見られることがある.

禁忌

1)妊婦または妊娠している可能性のある女性，低出生体重児，新生児，グルコース-6-リン酸脱水素酵素(G-6-PD)欠乏患者，本剤の成分またはサルファ剤に対し過敏症の既往歴のある患者.

2)ザルシタビン・ホスカルネットを投与中の患者，本剤に対する過敏症の既往歴のある患者.

吸入投与は，換気障害が重症の患者(PaO_2 60mmHg以下).

3)本剤に対する過敏症の既往歴のある患者.

解説

ニューモシスチス肺炎の治療は，効果発現の高さからST合剤が第1選択である．ST合剤はおもに過敏症と骨髄障害，ペンタミジンは腎機能障害や味覚障害や低血圧など，重篤な副作用の頻度が高く，使用にあたっては厳重な経過観察が必要である．一方の薬剤で副作用が見られた場合は，他方に切り替える．おおむね10日以上の治療が行われて改善が見られるものの，副作用などで両剤の投与が難しくなった場合には，ペンタミジンの吸入投与も用いることができる．ニューモシスチス肺炎の治療は21日間を原則とする.

ニューモシスチス肺炎治療では治療薬の投与とともに十分な副腎皮質ステロイドホルモンを開始して，治療に伴う過剰な炎症と，それによる肺の器質化を防止することが治療成功の鍵となる.

〈キーワード〉ノイラミニダーゼ　異常行動　骨髄障害　腎機能障害　吸入投与　副腎皮質ステロイドホルモン

研究成果の刊行に関する一覧表

平成 20 年度　国立感染症研究所　片野晴隆

雑誌

発表者氏名	論文タイトル名	発表誌名	巻号	ページ	出版年
Dewan, MZ, Takamatsu, N, Hidaka, T, Hatakeyama, K, Nakahata, S, Fujisawa, J, Katano, H, Yamamoto, N, Morishita, K.	Critical role for TSLC1 expression in the growth and organ infiltration of adult T-cell leukemia cells in vivo. J Virol.	J. Virol.	82	11958-11963	2008
Dewan, MZ, Tomita, M, Katano, H, Yamamoto, N, Ahmed, S, Yamamoto, M, Sata, T, Mori, N, Yamamoto, N.	An HIV protease inhibitor, ritonavir targets the nuclear factor-kappaB and inhibits the tumor growth and infiltration of EBV-positive lymphoblastoid B cells.	Int J Cancer.	124	622-629	2009

JOURNAL OF VIROLOGY, Dec. 2008, p. 11958–11963 Vol. 82, No. 23
0022-538X/08/$08.00+0 doi:10.1128/JVI.01149-08

NOTES

Critical Role for TSLC1 Expression in the Growth and Organ Infiltration of Adult T-Cell Leukemia Cells In Vivo▽

M. Zahidunnabi Dewan,[1,2]† Naofumi Takamatsu,[3] Tomonori Hidaka,[4] Kinta Hatakeyama,[5] Shingo Nakahata,[3] Jun-ichi Fujisawa,[6] Harutaka Katano,[7] Naoki Yamamoto,[1,2]* and Kazuhiro Morishita[3]*

Department of Molecular Virology, Graduate School, Tokyo Medical and Dental University, 1-5-45 Yushima, Bunkyo-ku, Tokyo 113-8519, Japan[1]; AIDS Research Center, National Institute of Infectious Disease, 1-23-1 Toyama, Shinjuku-ku, Tokyo 162-8640, Japan[2]; Department of Medical Sciences,[3] Department of Internal Medicine,[4] and Department of Pathology,[5] Faculty of Medicine, University of Miyazaki, Kiyotake, Miyazaki, Japan; Department of Microbiology, Kansai Medical University, Moriguchi, Osaka, Japan[6]; and Department of Pathology, National Institute of Infectious Diseases, 1-23-1 Toyama, Shinjuku-ku, Tokyo 162-8640, Japan[7]

Received 2 June 2008/Accepted 15 September 2008

Adult T-cell leukemia (ATL) is associated with human T-cell leukemia virus type 1 infection. The tumor suppressor lung cancer 1 (TSLC1) gene was previously identified as a novel cell surface marker for ATL, and this study demonstrated the involvement of TSLC1 expression in tumor growth and organ infiltration of ATL cells. In experiments using NOD/SCID/γc^{null} mice, both leukemia cell lines and primary ATL cells with high TSLC1 expression caused more tumor formation and aggressive infiltration of various organs of mice. Our results suggest that TSLC1 expression in ATL cells plays an important role in the growth and organ infiltration of ATL cells.

Human T-cell leukemia virus type 1 (HTLV-1) is the causative agent of an aggressive form of $CD4^+$ T-cell leukemia termed adult T-cell leukemia (ATL) (7, 14, 18). Carriers of HTLV-1 have been identified in a number of locations throughout the world, including parts of Africa; Papua New Guinea; specific regions in Europe including Romania; parts of South America including northern Brazil, Peru, northern Argentina, and Colombia; and the southern part of Kyushu in Japan (17). Common findings in patients with ATL include enlargement of peripheral lymph nodes, hepatomegaly, splenomegaly, skin infiltration, and hypercalcemia. The Tax gene is a unique viral gene thought to play a central role in HTLV-1-induced transformation. It is responsible for transactivation of the HTLV-1 long terminal repeat (5, 16) and numerous cellular genes involved in T-cell activation and growth, including those encoding interleukin-2 (IL-2) (11) and the α chain of IL-2 receptor (IL-2Rα) (CD25, Tac) (1, 2). The long latency of ATL development suggests that multiple genetic events accumulate in HTLV-1-infected cells; however, the precise molecular mechanisms of ATL leukemogenesis following HTLV-1 infection have not been fully elucidated.

The tumor suppressor lung cancer 1 gene (TSLC1) at chromosome 11q23 has been identified as a tumor suppressor gene in non-small-cell lung cancer (9, 13). In contrast, it was recently found to be highly and ectopically expressed in acute-type ATL cells, most ATL cell lines, and HTLV-1-infected T-cell lines (15). Enforced expression of TSLC1 in ATL-derived ED-40515(−) cells resulted in higher aggregations and binding abilities in a human umbilical vein endothelial cell line (HUVEC). These results suggest that TSLC1 might contribute to tumor growth by enhancing aggregation after infiltration and migration outside blood vessels. Since the role of TSLC1 overexpression in the course of tumor growth and organ infiltration of ATL cells remains to be fully elucidated, we investigated the direct involvement of TSLC1 in the growth and infiltration of leukemia cells using C57BL/6J and NOD-SCID/γc^{null} (NOG) mice (4, 8).

In order to analyze the tumorigenicity of TSLC1 expression in leukemia cells, a murine IL-2-independent T-lymphoma cell line (EL4) injected into the intraperitoneum of syngeneic C57BL/6J mice was used as a model for ATL. EL4 cells were transfected with a pcDNA3 expression plasmid containing TSLC1, and transformant cells were selected by a limiting-dilution method in the presence of G-418. We also used EL4 cells expressing a green fluorescent protein-Tax fusion protein (EL4/GAX) (6) and parental EL4 (EL4/p) as a control. Expression of Tax protein in EL4 cells, a 38-kDa band of Tax protein in HUT102 cells, and a 64-kDa band of green fluorescent protein-Tax fusion protein in EL4/GAX cells were all

* Corresponding author. Mailing address for Naoki Yamamoto: AIDS Research Center, National Institute of Infectious Disease, 1-23-1 Toyama, Shinjuku-ku, Tokyo 162-8640, Japan. Phone: 81-3-5285-1111. Fax: 81-3-5285-1165. E-mail: nyama@nih.go.jp. Mailing address for Kazuhiro Morishita: Division of Tumor and Cellular Biochemistry, Department of Medical Sciences, Faculty of Medicine, University of Miyazaki, Kiyotake, Miyazaki, Japan. Phone: 81-9-8585-0985. Fax: 81-9-8585-2401. E-mail: kmorishi@med.miyazaki-u.ac.jp.

† Present address: Department of Pathology, New York University School of Medicine, 550 First Avenue, New York, NY 10016.

▽ Published ahead of print on 15 October 2008.

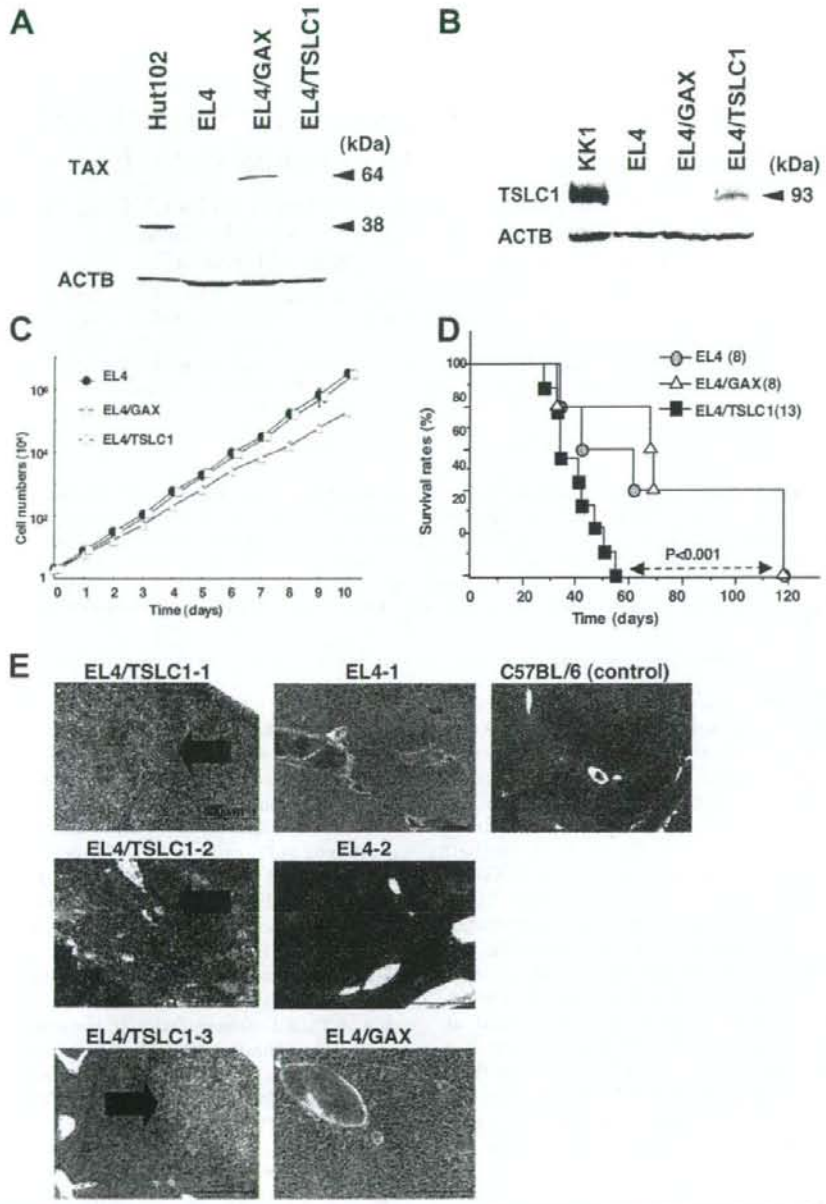

FIG. 1. Transplantation of EL4 T-cell lymphoma cells expressing TSLC1 shortened the life span of syngeneic mice. (A) Expression of Tax protein in HUT102, EL4, EL4/GAX, and EL4/TSLC1 cells was detected by Western blot analysis. Expression of β-actin protein (ACTB) was used as a loading control. (B) Expression of TSLC1 protein in KK1, EL4, EL4/GAX, and EL4/TSLC1 cells was detected by Western blot analysis. Expression of β-actin protein (ACTB) was used as a loading control. (C) Cell numbers in a growth curve are shown for an average of three independent counts, and standard deviations are indicated as error bars. (D) Survival curves of C57BL/6 mice inoculated in the abdominal cavity with EL4, EL4/GAX, or EL4/TSLC1 cells. Cumulative survival rates were calculated by the Kaplan-Meier method and compared using a log-rank test. (E) Liver sections from all mice were stained with hematoxylin-eosin. The regions of liver metastasis (arrow) were seen in liver sections from mice inoculated with EL4/TSLC1 cells but not shown in the liver sections from the mice inoculated with EL4 or EL4/GAX cells. Magnification, ×100; bars, 400 μm.

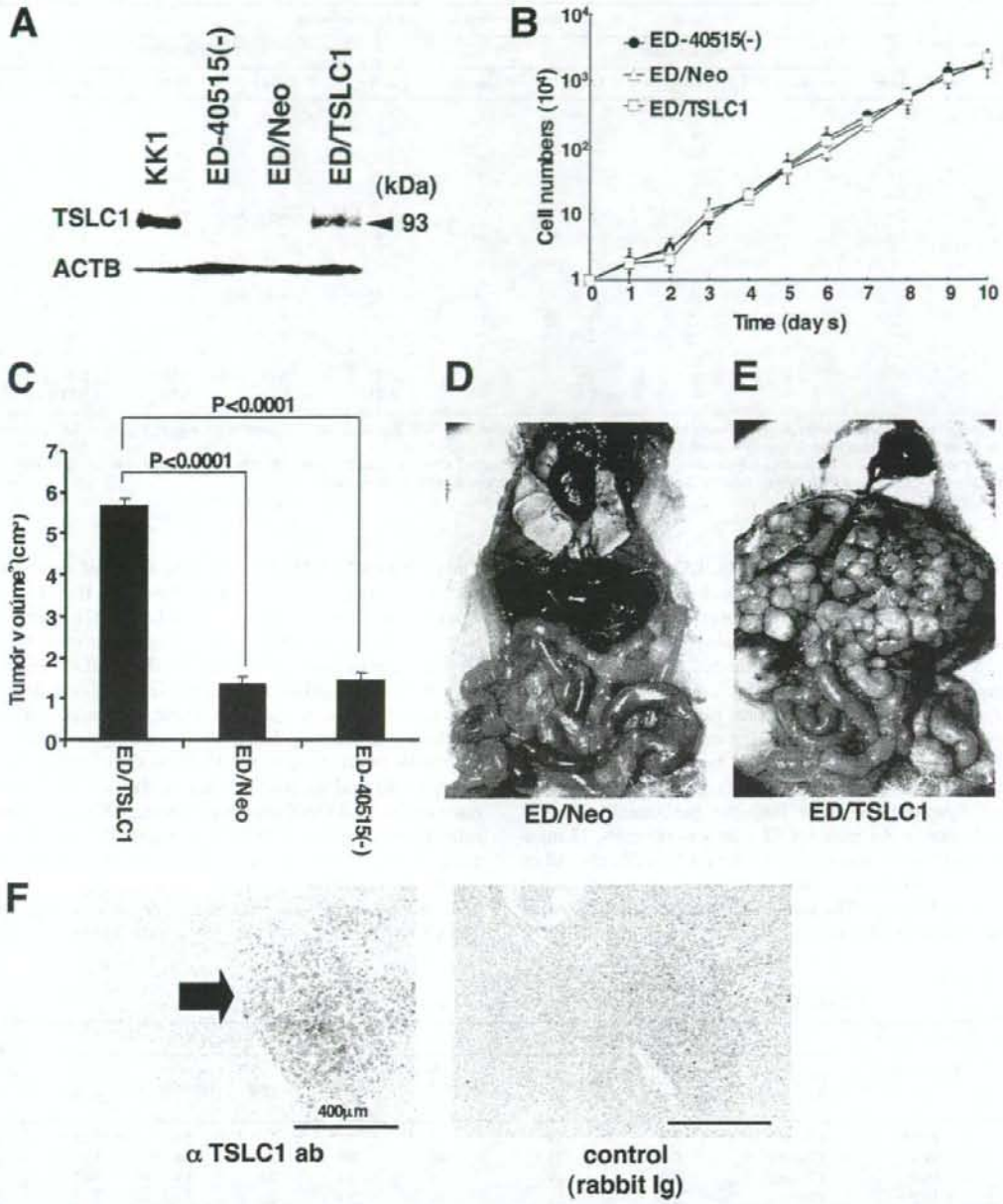

FIG. 2. Involvement of TSLC1 expression in tumor growth and infiltration of leukemia cells in NOG mice. (A) Expression of TSLC1 in KK1, ED-40515(−), ED/Neo, or ED/TSLC1 cell lines was detected by Western blot analysis. Expression of β-actin protein (ACTB) was used as a loading control. (B) Cell growth curves of ED-40515(−), ED/Neo, and ED/TSLC1 cell lines are shown for an average of three independent counts, and standard deviations are indicated as error bars. (C) Tumor volumes of mice inoculated subcutaneously with ED/TSLC1, ED/Neo, or ED-40515(−) cells after 21 days are shown as the means ± standard errors of the means for five mice in each group. Statistical analysis was done with a Student *t* test. (D and E) The pictures shown were derived from gross photographs of the sacrificed mice at 1 month after intravenous inoculation of ED/Neo (D) or ED/TSLC1 (E) cells. (F) Immunohistochemical staining for TSLC1 protein in liver metastases of the mice inoculated intravenously with ED/TSLC1 cells is shown. An arrow indicates a tumor mass with strong staining with a rabbit anti-TSLC1 antibody; however, the same mass shows no staining with rabbit immunoglobulin (Ig) as a negative control. Magnification, ×100; bars, 400 μm.

TABLE 1. Invasion scores of mice inoculated with ED/Neo or ED/TSLC1 cells

Cell line and mouse	Invasion score for organ by observation:									
	Macroscopic[a]					Microscopic[b]				
	Liver	Kidney	Lung	Ovary	Spleen	Liver	Kidney	Lung	Ovary	Spleen
ED/TSLC1										
T1	3+	−	+/−	1+	−	3+	−	2+	2+	−
T2	3+	−	−	1+	−	3+	−	2+	2+	−
T3	3+	−	+/−	2+	−	3+	−	2+	2+	−
T4	3+	−	−	1+	−	3+	−	2+	2+	−
T5	2+	−	−	2+	−	3+	−	2+	3+	−
T6	3+	−	+/−	1+	−	3+	−	+/−	2+	−
ED/Neo										
N1	−	−	−	2+	−	2+	−	+/−	3+	−
N2	+/−	−	−	1+	−	+/−	−	−	2+	−
N3	−	−	−	2+	−	−	−	+/−	2+	−
N4	−	−	−	1+	−	−	−	−	2+	−
N5	−	−	−	1+	−	ND[c]	ND	ND	ND	ND
N6	−	−	−	1+	−	ND	ND	ND	ND	ND

[a] Subjective invasion scores by macroscopic observation were as follows: −, no invasion; +/−, less than 10% invasion in the organ; 1+, 10 to 30% invasion in the organ; 2+, 30 to 70% invasion in the organ; 3+, over 70% invasion in the organ.
[b] Subjective invasion scores by microscopic observation were as follows: −, no invasion; +/−, less than 1% leukemia cells in the section; 1+, less than 10% leukemia cells in the section; 2+, 10 to 30% leukemia cells in the section; 3+, over 30% leukemia cells in the section
[c] ND, not done.

detected by Western blot analysis (Fig. 1A). Expression of a TSLC1 protein in EL4/TSLC1 cells was also shown on Western blot analysis with KK1, an ATL cell line expressing TSLC1 (12) (Fig. 1B). In an in vitro cell growth assay, 2×10^4 cells were incubated, and their growth was analyzed by direct counting with trypan blue dye staining. EL4 and EL4/TSLC1 cells showed nearly identical proliferation profiles in vitro, while Tax-expressing EL4 cells proliferated more slowly (Fig. 1C). This difference in cell growth might be caused by different expression vectors. In an in vivo growth assay, 2×10^6 cells of each cell line were injected into the peritoneal cavity of C57BL/6J mice: eight mice for EL4 cells as controls, 13 mice for EL4/TSLC1 cells, and eight mice for EL4/GAX cells. All of the mice died of tumor invasion of various organs with ascitic fluids in 40 to 120 days. The median survival time of the control mice injected with EL4 cells or EL4/GAX cells was 72 days. The mice with EL4/TSLC1 cells, however, died within 60 days, with a median survival time of 41 days (Fig. 1D). The phenotypes of the control mice and the EL4/TSLC1 mice were almost identical with invasion of tumors into various organs. Organ metastasis of tumor cells in three EL4/TSLC1-inoculated mice, two EL4-inoculated mice, and one EL4/GAX-inoculated mouse was analyzed and evaluated with hematoxylin-eosin staining. The liver was one of the major sites of metastasis in all three of the EL4/TSLC1-inoculated mice by histopathological analysis but not in the two EL4-inoculated mice or the EL4/GAX-inoculated mouse (Fig. 1E). These results support the role of TSLC1 overexpression in T-lymphoma cells as one of an aggressive factor in the development of leukemia/lymphoma.

In order to investigate the possibility that overexpression of TSLC1 promotes tumor growth and/or infiltration in vivo,

TABLE 2. Clinical characteristics of patients and pathological findings of organ invasion[a]

Patient no.	Age (yr)/sex	Clinical characteristic				Invasion score in NOG mice[b]				TSLC1 expression score[c]
		Diagnosis (ATL type)	WBC (10^9/liter)	Lymphocytes (%)	Atypical cells (%)	Liver	Lung	Spleen	Lymph node	
1	73/M	Chronic	7.8	59	47	3+	3+	3+	ND	3+
2	59/F	Chronic	9.0	75	40	3+	2+	2+	1+	2+
3	66/F	Chronic	29.4	49	75	3+	3+	3+	ND	3+
4	44/F	Chronic	22.6	51	45	3+	2+	2+	2+	2+
5	43/F	Chronic	18.6	63	43	3+	3+	3+	ND	2+
6	54/M	Acute	192.8	65	91	1+	2+	ND	ND	1+
7	58/M	Acute	67.3	71	80	3+	3+	3+	ND	2+
8	65/F	Acute	29.4	25	60	3+	2+	ND	3+	3+
9	68/M	Acute	30.0	79	81	3+	1+	1+	2+	2+
10	66/F	Acute	10.2	38	51	3+	3+	3+	ND	3+

[a] Abbreviations: M, male; F, female; WBC, white blood cells; ND, not done.
[b] Subjective invasion scores were as follows; 0, no invasion; 1+, less than 10% leukemia cells in the section; 2+, 10 to 30% leukemia cells in the section; 3+, over 30% leukemia cells in the section.
[c] Subjective scores of TSLC1 expression in pathological immunostaining were as follows; −, no staining; 1+, faint staining in less than 10% of invasive leukemia cells; 2+, weak to moderate staining in 30 to 70% of invasive leukemia cells; 3+, intense staining in more than 70% of invasive leukemia cells.

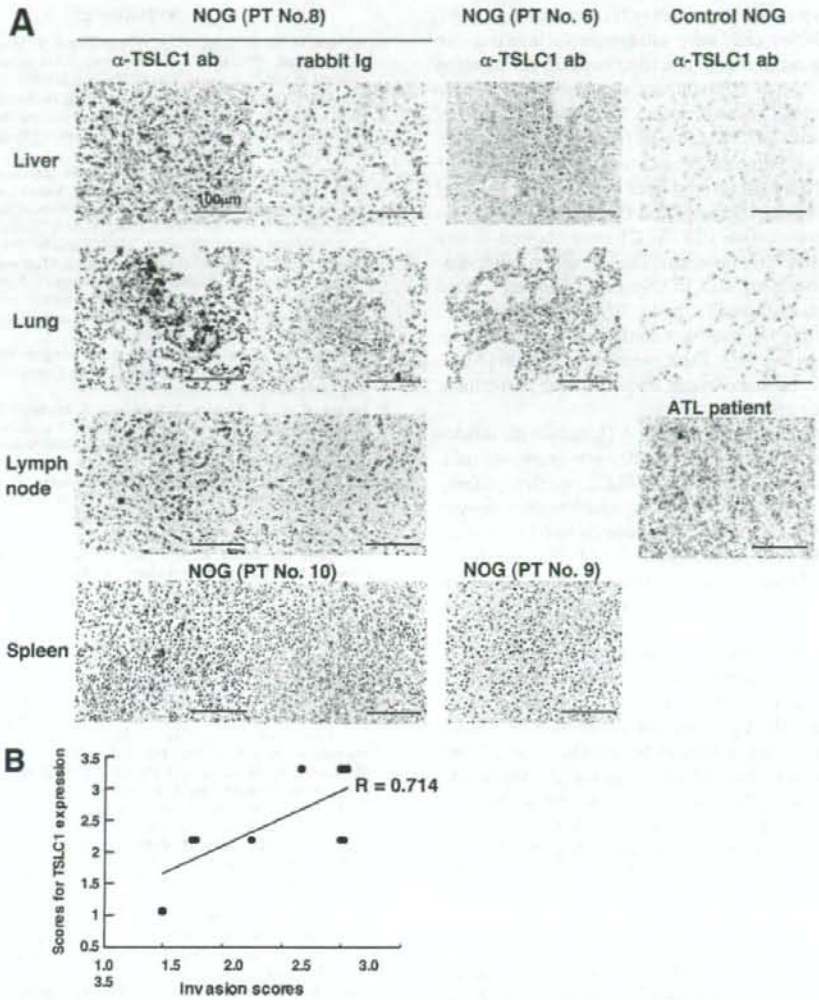

FIG. 3. Growth and infiltration of primary ATL cells in various organs of NOG mice based on TSLC1 expression. (A) Immunohistochemical staining of various organs of NOG mice inoculated with leukemia cells from patient 6, 8, 9, or 10 is shown with the use of rabbit anti-TSLC1 antibody or rabbit immunoglobulin (Ig) as a negative control. Sections from patients 8 and 10 showed severe invasion (invasion score, 3) and dense staining for TSLC1 (expression score, 3), while sections from patients 6 and 9 showed mild invasion (invasion score, 1) and light staining for TSLC1 (expression score, 1). Liver and lung sections from control NOG mice were used as negative controls, and a lymph node from an ATL patient was used as a positive control. Magnification, ×400; bars, 100 μm. (B) The diagram of dispersion between mean values of each invasion score and scores for TSLC1 expression in each NOG mouse inoculated with primary ATL cells showed moderate correlation ($R = 0.714$).

ATL-derived ED-40515(−) cells (10) were injected into NOG mice. Since expression of TSLC1 in ED-40515(−) cells is severely reduced by promoter methylation, they were transfected with either a TSLC1 expression plasmid (pcDNA3/TSLC1) or a mock plasmid (pcDNA3/Neo). ED/TSLC1 and ED/Neo cells were identified by selection with G-418. High levels of TSLC1 expression were verified in the ED/TSLC1 cells, but not in the ED/Neo cells, by Western blot analysis (Fig. 2A). The ED/TSLC1, ED/Neo, and ED-40515(−) cell lines all showed the same proliferation profile in vitro (Fig. 2B). Cells (10×10^6) were inoculated subcutaneously into the postauricular region of NOG mice, which permitted the observation of tumor growth macroscopically and the measurement of tumor size over a relatively short time (3). The ED/TSLC1 cell lines caused greater formation of larger tumors than did the ED/Neo and ED-40515(−) cell lines (Fig. 2C). The development of clinical signs of near-death (e.g., piloerection, weight loss, and cachexia) in mice at the time of killing was also more prevalent with the ED/TSLC1 cell line. These results suggest that TSLC1 expression in ATL cells enhances in vivo tumor growth in NOG mice.

Since the mice died within 4 weeks after subcutaneous in-

oculation of leukemia cells due to heavy tumor burden, 2×10^6 ED/TSLC1 or ED/Neo cells were intravenously injected into six NOG mice in order to investigate their capacity for invasion of various organs. After 1 month, we sacrificed the mice to determine the extent of organ invasion. Macroscopically, all of the mice injected with ED/TSLC1 cells (six/six) showed severe liver invasion with swelling of the ovaries. None of the mice injected with ED/Neo cells showed liver invasion, but they did show ovarian involvement (Fig. 2D and E). Microscopically, all of the mice inoculated with ED/TSLC1 cells showed severe and massive liver and lung invasions. On the other hand, only one of six mice inoculated with ED/Neo cells showed a large amount of liver metastasis (Table 1). TSLC1 expression in tumor cells infiltrating the liver was confirmed by immunohistochemical staining (Fig. 2F). Thus, overexpression of TSLC1 in ATL cells might enhance organ invasion, and particularly invasion of the liver and lung.

Next, we examined whether primary ATL cells with various levels of expression of TSLC1 could efficiently grow and infiltrate various organs in NOG mice. TSLC1-positive primary ATL cells (2×10^7) from five acute-type and five chronic-type ATL patients were inoculated subcutaneously into the postauricular region of NOG mice (Table 2). All of the mice developed clinical signs of near-death (e.g., piloerection, weight loss, and cachexia) 6 to 8 weeks after inoculation, in addition to the enlargement of the lymph nodes, spleen, lungs, and liver. Microscopically, ATL cells invaded various organs of all ATL-bearing NOG mice to different degrees. Based on results of immunohistochemical staining for TSLC1, all invading leukemia cells expressed TSLC1 protein, compared with no TSLC1 expression in these organs in control NOG mice (Table 2 and Fig. 3A). The dispersion diagram for the levels of invasion and the levels of TSLC1 expression in the leukemia cells showed a correlation coefficient of 0.714, suggesting that there was a moderate correlation between invasive capability and the level of TSLC1 expression (Fig. 3B). Thus, TSLC1 could aid in the formation of a rapidly growing large tumor and massive infiltration of ATL cells into various organs in NOG mice. Since TSLC1 is expressed in various types of ATL cells, including smoldering and chronic types, it might be a promising target for the development of a new anti-ATL therapy. The NOG mouse model system described in the present study could provide a novel means by which to understand and investigate the further importance of TSLC1 in ATL progression.

We thank S. Ichinose of the Instrumental Analysis Research Center; S. Endo of the Animal Research Center, Tokyo Medical and Dental University; and Y. Sato of the National Institute of Infectious Diseases for her excellent technical assistance. Anti-Tax (MI73) antibody was the kind gift of Y. Namba and M. Matsuoka (Institute for Virus Research, Kyoto University).

Supported by grants from the Ministry of Education, Science, and Culture; the Ministry of Health, Labor, and Welfare; and Human Health Science of Japan.

REFERENCES

1. **Ballard, D. W., E. Bohnlein, J. W. Lowenthal, Y. Wano, B. R. Franza, and W. C. Greene.** 1988. HTLV-I tax induces cellular proteins that activate the B element in the IL-2 receptor gene. Science **241:**1652–1655.
2. **Cross, S. L., M. B. Feinberg, J. B. Wolf, N. J. Holbrook, F. Wong-Staal, and W. J. Leonard.** 1987. Regulation of the human interleukin-2 receptor chain promoter: activation of a nonfunctional promoter by the transactivator gene of HTLV-I. Cell **49:**47–56.
3. **Dewan, M. Z., K. Terashima, M. Taruishi, H. Hasegawa, M. Ito, Y. Tanaka, N. Mori, T. Sata, Y. Koyanagi, M. Maeda, Y. Kubuki, A. Okayama, M. Fujii, and N. Yamamoto.** 2003. Rapid tumor formation of human T-cell leukemia virus type 1-infected cell lines in novel NOD-SCID/$c\gamma^{null}$ mice: suppression by an inhibitor against NF-κB. J. Virol. **77:**5286–5294.
4. **Dewan, M. Z., J. N. Uchihara, K. Terashima, M. Honda, T. Sata, M. Ito, N. Fujii, K. Uozumi, K. Tsukasaki, M. Tomonaga, Y. Kubuki, A. Okayama, M. Toi, N. Mori, and N. Yamamoto.** 2006. Efficient intervention of growth and infiltration of primary adult T-cell leukemia cells by an HIV protease inhibitor, ritonavir. Blood **107:**716–724.
5. **Felber, B. K., H. Paskalis, C. Kleinman-Ewing, F. Wong-Staal, and G. N. Pavlakis.** 1985. The pX protein of HTLV-I is a transcriptional activator of its long terminal repeats. Science **229:**675–679.
6. **Furuta, R. A., K. Sugiura, S. Kawakita, T. Inada, S. Ikehara, T. Matsuda, and J. Fujisawa.** 2002. Mouse model for the equilibration interaction between the host immune system and human T-cell leukemia virus type 1 gene expression. J. Virol. **76:**2703–2713.
7. **Hinuma, Y., K. Nagata, M. Hanaoka, M. Nakai, T. Matsumoto, K. I. Kinoshita, S. Shirakawa, and I. Miyoshi.** 1981. Adult T-cell leukemia: antigen in an ATL cell line and detection of antibodies to the antigen in human sera. Proc. Natl. Acad. Sci. USA **78:**6476–6480.
8. **Ito, M., H. Hiramatsu, K. Kobayashi, K. Suzue, M. Kawahata, K. Hioki, Y. Ueyama, Y. Koyanagi, K. Sugamura, K. Tsuji, T. Heike, and T. Nakahata.** 2002. NOD/SCID/.cnull mouse: an excellent recipient mouse model for engraftment of human cells. Blood **100:**3175–3182.
9. **Kuramochi, M., H. Fukuhara, T. Nobukuni, T. Kanbe, T. Maruyama, H. P. Ghosh, M. Pletcher, M. Isomura, M. Onizuka, T. Kitamura, T. Sekiya, R. H. Reeves, and Y. Murakami.** 2001. TSLC1 is a tumor suppressor gene in human non-small cell lung cancer. Nat. Genet. **27:**427–730.
10. **Maeda, M., A. Shimizu, K. Ikuta, H. Okamoto, M. Kashihara, T. Uchiyama, T. Honjo, and J. Yodoi.** 1985. Origin of human T-lymphotrophic virus I-positive T cell lines in adult T cell leukemia. Analysis of T cell receptor gene rearrangement. J. Exp. Med. **162:**2169–2174.
11. **Maruyama, M., H. Shibuya, H. Harada, M. Hatakeyama, M. Seiki, T. Fujita, J. Inoue, M. Yoshida, and T. Taniguchi.** 1987. Evidence for aberrant activation of the interleukin-2 autocrine loop by HTLV-1-encoded p40x and T3/Ti complex triggering. Cell **48:**343–350.
12. **Masuda, M., M. Yagita, H. Fukuhara, M. Kuramochi, T. Maruyama, A. Nomoto, and Y. Murakami.** 2002. The tumor suppressor protein TSLC1 is involved in cell-cell adhesion J. Biol. Chem. **277:**31014–31019.
13. **Murakami, Y., T. Nobukuni, K. Tamura, T. Maruyama, T. Sekiya, Y. Arai, H. Gomyou, A. Tanigami, M. Ohki, D. Cabin, P. Frischmeyer, P. Hunt, and R. H. Reeves.** 1998. Localization of tumor suppressor activity important in non-small cell lung carcinoma on chromosome 11q. Proc. Natl. Acad. Sci. USA **95:**8153–8158.
14. **Poiesz, B. J., F. W. Ruscetti, A. F. Gazdar, P. A. Bunn, J. D. Minna, and R. C. Gallo.** 1980. Detection and isolation of type C retrovirus particles from fresh and cultured lymphocytes of a patient with cutaneous T-cell lymphoma. Proc. Natl. Acad. Sci. USA **77:**7415–7419.
15. **Sasaki, H., I. Nishikata, T. Shiraga, E. Akamatsu, T. Fukami, T. Hidaka, Y. Kubuki, A. Okayama, K. Hamada, H. Okabe, Y. Murakami, H. Tsubouchi, and K. Morishita.** 2005. Overexpression of a cell adhesion molecule, TSLC1, as a possible molecular marker for acute type of adult T-cell leukemia. Blood **105:**1204–1213.
16. **Sodroski, J. G., C. A. Rosen, and W. A. Haseltine.** 1984. Transacting transcriptional activation of the long terminal repeat of human T lymphotropic viruses in infected cells. Science **225:**381–385.
17. **Yamaguchi, K., and T. Watanabe.** 2002. Human T lymphotropic virus type-I and adult T-cell leukemia in Japan. Int. J. Hematol. **76:**240–245.
18. **Yoshida, M., I. Miyoshi, and Y. Hinuma.** 1982. Isolation and characterization of retrovirus from cell lines of human adult T-cell leukemia and its implication in the disease. Proc. Natl. Acad. Sci. USA **79:**2031–2035.

Int. J. Cancer: **124,** 622–629 (2009)

An HIV protease inhibitor, ritonavir targets the nuclear factor-kappaB and inhibits the tumor growth and infiltration of EBV-positive lymphoblastoid B cells

Md. Zahidunnabi Dewan[1,2], Mariko Tomita[3], Harutaka Katano[4], Norio Yamamoto[1], Sunjida Ahmed[1], Michiko Yamamoto[5], Tetsutaro Sata[4], Naoki Mori[3]* and Naoki Yamamoto[1,2]*

[1]*Department of Molecular Virology, Graduate School, Tokyo Medical and Dental University, 1-5-45 Yushima, Bunkyo-ku, Tokyo 113-8519, Japan*
[2]*AIDS Research Center, National Institute of Infectious Diseases, 1-23-1 Toyama, Shinjuku-ku, Tokyo 162-8640, Japan*
[3]*Division of Molecular Virology and Oncology, Graduate School of Medicine, University of the Ryukyus, 207 Uehara, Nishihara, Okinawa 903-0215, Japan*
[4]*Department of Pathology, National Institute of Infectious Diseases, 1-23-1 Toyama, Shinjyuku-ku, Tokyo 162-8640, Japan*
[5]*Division of Safety Information on Drug, National Institute of Health Sciences, Food and Chemicals, Setagaya-ku, Tokyo 158-8501, Japan*

Epstein-Barr Virus (EBV)-associated immunoblastic lymphoma occurs in immunocompromised patients such as those with AIDS or transplant recipients after primary EBV infection or reactivation of a preexisting latent EBV infection. In the present study, we evaluated the effect of ritonavir, an HIV protease inhibitor, on EBV-positive lymphoblastoid B cells *in vitro* and in mice model. We found that it induced cell-cycle arrest at G_1-phase and apoptosis through down-regulation of cell-cycle gene cyclin D2 and anti-apoptotic gene survivin. Furthermore, ritonavir suppressed transcriptional activation of NF-κB in these cells. Ritonavir efficiently prevented growth and infiltration of lymphoma cells in various organs of NOD/SCID/γc^{null} mice at the same dose used for treatment of patients with AIDS. Our results indicate that ritonavir targets NF-κB activated in tumor cells and shows anti-tumor effects. These data also suggest that this compound may have promise for treatment or prevention of EBV-associated lymphoproliferative diseases that occur in immunocompromised patients.

Key words: ritonavir; LCLs; NF-κB; NOG mice

Epstein-Barr virus (EBV) is a ubiquitous human γ herpes virus that establishes a latent infection more than 90% of adults worldwide.[1] Immunocompromised individuals such as those with AIDS or transplant recipients are at increased risk for developing aggressive EBV-associated lymphoproliferative diseases. EBV is associated with malignant diseases, including Burkitt's lymphoma,[1,2] nasopharyngeal carcinoma[3,4] and immunoblastic B cell lymphoma of immunosuppressed individuals. Infection of primary B cells with EBV results in transformation with growth of the cells in tight clumps and immortalization of the cells. These immortalized B cells have an immunoblastic morphology and express each of the EBV-encoded small RNAs (EBERs), EBV nuclear antigen (EBNAs) and latent membrane proteins (LMPs).[2,5] EBERs have oncogenic potential through inhibition of PKR.[6] EBNA-2 is a transactivator that up-regulates expression of cellular genes and LMPs. LMP-1 may mediate proliferative and survival effects not only in EBV-transformed B lymphocytes but also in these malignancies that occur long after primary infection. Many immunocompromised patients with EBV-associated immunoblastic lymphoma have tumors at extranodal sites such as the brain, lung, or gastrointestinal tract. The prognosis of EBV-associated lymphomas is very poor for patients with irreversible immunosuppression and treatment options are limited.

Despite the diversity in clinical manifestations of hematopoietic malignancies, strong and constitutive nuclear factor-kappaB (NF-κB) activation was reported to be a unique and common characteristic of malignant cells.[7,8] In resting cells, NF-κB is sequestered as an inactive precursor by association with inhibitory IκBs in the cytoplasm. On stimulation, IκBs are rapidly phosphorylated, ubiquitinated and degraded by a proteasome-dependent pathway allowing active NF-κB to translocate into the nucleus where it can activate the expression of a number of genes.[9] LMP-1 is an oncoprotein that constitutively activates NF-κB to induce B cell proliferation.[7] Lymphoblastoid cell lines (LCLs) express high level of the antiapoptotic proteins BCL-2, BCL-xL, c-IAP1, Bfl-1 and c-FLIP the targets of NF-κB.[10,11] NF-κB activation has been connected with multiple processes of oncogenesis including control of apoptosis, cell-cycle, differentiation and cell migration,[9] and therefore, inhibition of NF-κB was suggested to be a useful strategy for cancer therapy.[12–20] It has been also reported that inhibition of NF-κB in EBV-associated lymphomas results in induction of apoptosis.[21] Therefore, targeting the NF-κB pathway and inhibition of NF-κB activity is a logical strategy for treating EBV-associated lymphomas.

Ritonavir, a human immunodeficiency virus type 1(HIV-1) protease inhibitor, has been successfully used in clinical treatments of HIV infection, with patients exhibiting a marked decrease in HIV viral load and a subsequent increase in $CD4^+$ T-cell counts.[22–25] Evidence of other effects by ritonavir on cellular proteases, such as the cysteine proteases cathepsin D and E, was presented in the drug's original description, albeit at concentrations >500-fold above the concentration required for inhibition of HIV protease.[26] Protease inhibitors have also been shown to directly affect cell metabolism, interfere with host or fungal proteases and block T-cell activation and dendritic-cell function.[27,28] Ritonavir has been shown to inhibit the chymotrypsin-like activity of the 20S proteasome, and it activates the chymotrypsin-like activity of the 26S proteasome conversely.[27,29,30] Ritonavir also has been reported to inhibit the transactivation of NF-κB induced by activators such as TNFα, HIV-1 Tat protein and the human herpesvirus 8 protein ORF74.[31] It is possible that inhibition of NF-κB activation by ritonavir is linked to additional pathways other than inhibition of proteasome.[31] Protease inhibitors also have been shown to have direct antiangiogenic and antitumor activity.[31,32] Recently, we reported that ritonavir inhibits growth and infiltration of ATL cells through targeting NF-κB.[20]

Grant sponsors: Ministry of Education, Science and Culture, The Ministry of Health, Labor and Welfare, Human Health Science of Japan.
Md. Zahidunnabi Dewan's current address is: Department of Pathology, New York University School of Medicine, 550 First Avenue, New York, NY 10016, USA.
Md. Zahidunnabi Dewan and Mariko Tomita contributed equally to this work.
***Correspondence to:** AIDS Research Center, National Institute of Infectious Diseases, 1-23-1 Toyama, Shinjuku-ku, Tokyo 162-8640, Japan. Fax: 8135-285-1165. E-mail: nyama@nih.go.jp (or) Division of Molecular Virology and Oncology, Graduate School of Medicine, University of the Ryukyus, 207 Uehara, Nishihara, Okinawa 903-0215, Japan.
Fax: 81-98-895-1410. E-mail: n-mori@med.u-ryukyu.ac.jp.
Received 14 July 2008; Accepted after revision 2 September 2008
DOI 10.1002/ijc.23993
Published online 15 September 2008 in Wiley InterScience (www.interscience.wiley.com).

Publication of the International Union Against Cancer

In the present, we demonstrate that inhibition of NF-κB activity by ritonavir results in marked increase of apoptosis and induce cell-cycle arrest in EBV-positive lymphoblastoid B cells. We found that ritonavir also suppresses the expression of genes involved in antiapoptosis and cell-cycle progression. In addition, we established preclinical models using newly developed NOD/SCID/γc^{null} (NOG) mouse.[16] a unique type of animal, lacking T-, B- and NK-cells to evaluate the efficacy of antitumor and anti-NF-κB therapies. In the murine model, ritonavir at the clinically relevant dose potently inhibited the growth and infiltration of EBV-transformed LCL cells.

Material and methods

Mice and cells

NOG mice were obtained from the Central Institute for Experimental Animals (Kawasaki, Japan). All mice were maintained under specific-pathogen-free conditions in the Animal Center of Tokyo Medical and Dental University (Tokyo, Japan). The Ethical Review Committee of the Institute approved the experimental protocol.

EBV-positive immortalized lymphoblatoid B-cell lines (LCL-Ya, LCL-Ao, LCL-Ka and LCL-Ku) were cultured in RPMI 1640 medium supplemented with 10% heat-inactivated fetal bovine serum (JRH Biosciences, Lenexa, KS), 100 U/ml penicillin, and 10 μg/ml streptomycin. Peripheral blood mononuclear cells (PBMCs) from 3 healthy volunteers were analyzed. Mononuclear cells were isolated by Ficoll-Paque density gradient centrifugation (GE Healthcare Biosciences, Uppsala, Sweden) and washed with PBS.

Cell viability assay

The effect of ritonavir on cell viability of LCLs and PBMCs from healthy donors was examined by the reagent, water-soluble tetrazolium (WST)-8 (Wako Chemicals, Osaka, Japan). Briefly, 2×10^5 cells were incubated in a 96-well microculture plate in the absence or presence of various concentrations of ritonavir. After 72 hr of culture, WST-8 (5 μl) was added for the last 4 hr of incubation and absorbance at 450 nm was measured using an automated microplate reader. Measurement of mitochondrial dehydrogenase cleavage of WST-8 to formazan dye provides an indication of the level of cell viability.

Cell-cycle analysis

Cells were plated at a density of 3×10^5/ml in 60-mm tissue culture dishes. Twelve hours after plating, cells were exposed to 40 μM ritonavir for 24 h. Cell-cycle analysis was performed with the CycleTEST PLUS DNA reagent kit (Becton Dickinson, San Jose, CA). Briefly, cells were washed with a buffer solution containing sodium citrate, sucrose and dimethyl sulfoxide, suspended in a solution containing RNase A, and stained with 125 μg/ml propidium iodide (PI) for 10 min. Cell suspensions were analyzed on EPICS XL flow cytometer (Beckman Coulter, Fullerton, CA) using EXPO32 software. The cell population at each cell-cycle phase was determined with MultiCycle software (Beckman Coulter).

Assay for apoptosis

Cells were plated at a density of 3×10^5/ml in 60-mm tissue culture dishes. Twelve hours after plating, cells were exposed to ritonavir for 72 hr. Apoptosis was quantified by double staining with Annexin-V-Fluos (Roche Diagnostics, Mannheim, Germany) and PI (Backman Coulter) according to the instructions supplied by the manufacturer. Cells were analyzed on EPICS XL flow cytometer (Beckman Coulter) using EXPO32 software.

Western blot analysis

Treated cells were solubilized at 4°C in lysis buffer containing 62.5 mM Tris-HCl (pH 6.8), 2% SDS, 10% glycerol, 6% 2-mercaptoethanol and 0.01% bromophenol blue. Samples were subjected to electrophoresis on SDS-polyacrylamide gels followed by transfer to a polyvinylidine difluoride membrane and probing with the following specific antibodies: polyclonal antibodies against survivin, cyclin D2 (Santa Cruz Biotechnology, Santa Cruz, CA), Bcl-X_L (BD Transduction Laboratories, San Jose, CA) and monoclonal antibodies against Bcl-2, p53, actin (NeoMarkers, Fremont, CA), PARP (BD Transduction Laboratories) and LMP-1 (DAKO, Kyoto, Japan). The protein bands recognized by the antibodies were visualized using the enhanced chemiluminescence system (Amersham, Piscataway, NJ).

Electrophoresis mobility shift assay (EMSA)

Cells were placed in culture at 1×10^6 cells/ml and examined for inhibition of NF-κB 24 hr after exposure to ritonavir. Nuclear proteins were extracted, and NF-κB binding activities to κB element were examined by EMSA as described previously.[8] In brief, 5 μg of nuclear extracts were preincubated in a binding buffer containing 1 μg of poly (dI:dC) (Amersham Biosciences), followed by addition of ^{32}P-labeled oligonucleotide probe containing NF-κB element (5×10^4 c.p.m.). These mixtures were incubated for 15 min at room temperature. The DNA-protein complexes were separated on a 4% polyacrylamide gel and visualized by autoradiography. To examine the specificity of the NF-κB element probe, unlabeled competitor oligonucleotides were preincubated with nuclear extracts for 15 min before incubation with probes. The probe or competitors used were prepared by annealing the sense and antisense synthetic oligonucleotides as follows: a typical NF-κB element from the *IL-2Rα* gene, 5′-gatcCGGCAGGGGAATCTCCCTCTC-3′; and AP-1 element of the *IL-8* gene, 5′-gactGTGATGACTCAGGTT-3′. Underlined sequences represent the NF-κB or AP-1 binding site. To identify NF-κB protein in the DNA protein complex revealed by EMSA, we used antibodies specific for various NF-κB proteins, including p50, p65, c-Rel, RelB and p52 (Santa Cruz Biotechnology), to elicit a supershift DNA protein complex formation. These antibodies were incubated with the nuclear extracts for 45 min at room temperature before incubation with radiolabeled probes.

Inoculation of EBV-positive immortalized LCLs and collection of samples

LCL Cells [LCL-Ya, LCL-Ao, LCL-Ka and LCL-Ku] were washed twice with serum-free RPMI-1640 medium and resuspended in same medium. Mice were anaesthetized with ether and cells were inoculated subcutaneously (sc) in the postauricular region of NOG mice at a dose of 1×10^7 cells per mouse. All mice were sacrificed 3 weeks after inoculation with lymphoma cells. We measured tumor size 3 weeks after inoculation. Tissues and various organs of mice were collected and fixed with Streck Tissue Fixative, then processed to paraffin wax-embedded sections for staining with hematoxylin and eosin (HE) and immunostaining.

PCR primer and conditions

Detection of the BamHI W repeat region of the EBV genome was performed using 100 ng of genomic DNA extracted from LCLs as follows. LCLs were lysed with genomic DNA extraction buffer (100 mM Tris-HCl pH8.0, 5 mM EDTA, 0.2% SDS, 200 mM NaCl and 200 μg/mL proteinase K) and the lysate was incubated at 50°C for 3 hr. After phenol-chloroform extraction, genomic DNA was purified by ethanol precipitation procedure. A 121-bp fragment of the EBV W repeat region was amplified by the forward primer 5′-CGCATAATGGCGGACCTAG-3′ and reverse primer 5′-CAAACAAGCCCACTCCCC-3′ in a 25 μl reaction mixture comprising 1 × AmpliTaq Gold buffer, 3.5 mM MgCl2, 200 μM dNTP, 300 nM primers, 200 nM probe and 0.025 U/μl AmpliTaq Gold. The PCR cycle conditions were as follows: a DNA denaturation and polymerase activation step of 10 min at 95°C and then 40 cycles of amplification (95°C for 15 sec, 60°C for 1 min). PCR products were separated by electrophoresis on agarose gels, stained with ethidium bromide and visualized by UV-light.

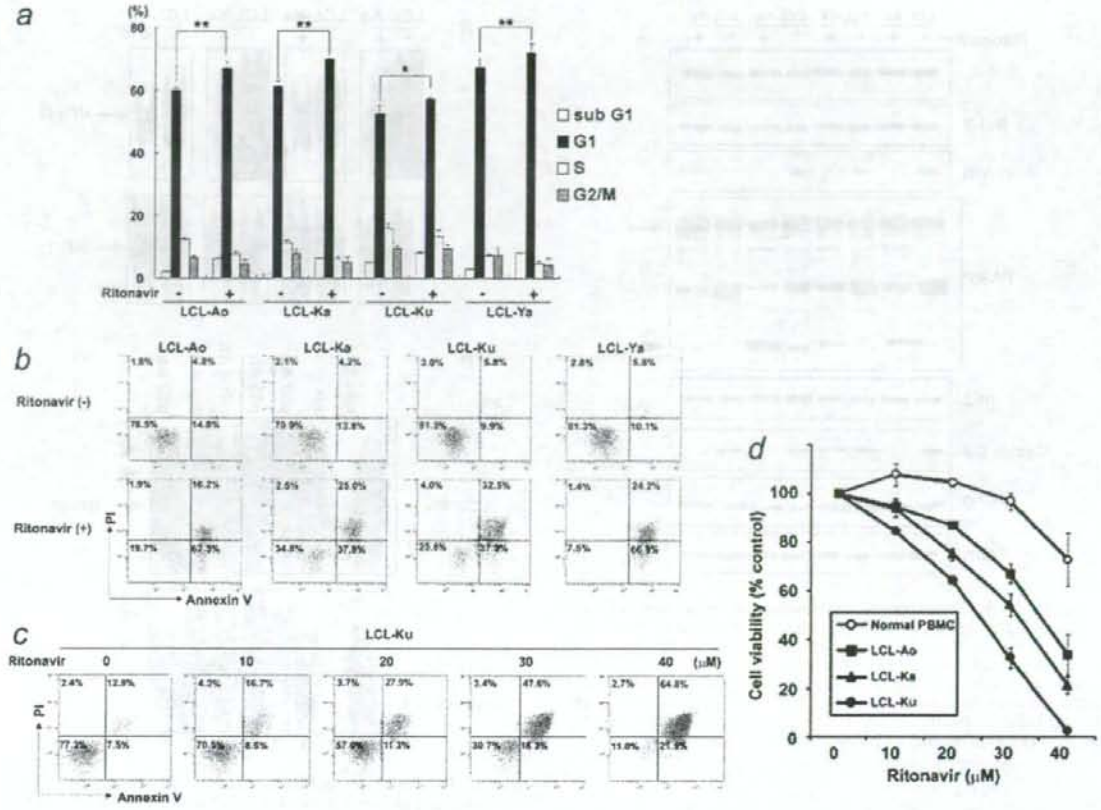

FIGURE 1 – Effect of ritonavir on cell cycle arrest and induction of apoptosis of EBV-positive lymphoblastoid B cells. (*a*) Effect of ritonavir on cell cycle progression of EBV-positive lymphoblastoid B cells. Cells were cultured for 24 hr with (+) or without (−) ritonavir (40 μM). DNA content was analyzed by flow cytometry with PI staining. Sub G_1, S and G_2/M indicate the stages of the cell cycle. Data are expressed as the mean percentages of the cells from three independent experements. Significance of differences between % G_1 of ritonavir treated (+) and untreated (−) cells calculated by Student's *t*-test is shown as *P*-value with astalisk(s). $^*p < 0.05$ and $^{**}p < 0.01$. (*b*) Effect of ritonavir on induction of apoptosis of EBV-immortalized B-cell lines. Cells were cultured for 72 hr with (+) or without (−) ritonavir (40 μM). (*c*) Ritonavir induces apoptosis of EBV-immortalized B-cell lines in a dose-dependent manner. LCL-Ku cells were cultured for 72 hr with increasing concentration of ritonavir (0, 10, 20, 30, 40 μM). Cells were harvested and stained with Annexin-V and PI. Apoptosis was analyzed by flow cytometry. Bottom left quadrants, viable cells; bottom right quadrants, early apoptotic cells. Top right quadrants, nonviable, late apoptotic/necrotic cells. (*d*) Effect of ritonavir on cell viability of LCLs and PBMCs from normal healthy controls. LCLs and PBMCs were incubated in the presence of various concentrations of ritonavir for 72 hr and viability of the cultured cells was measured by WST-8 assay. Relative viability of the cultured cells is presented as the mean determined on LCLs and PBMCs from triplicate cultures. A relative viability of 100% was designated as total number of cells that grew in 72-hr cultures in the absence of ritonavir.

Treatment of tumor-bearing mice with ritonavir

Ritonavir was obtained from Abbott Labs, North Chicago, IL. LCL-Ku cells (1×10^7) were inoculated s.c. in the post-auricular region of NOG mice. The drug was administered s.c. into the tumor cells inoculated site of mice at doses of 30 mg/kg/day, beginning on day 0 for 3 weeks. The control mice received RPMI-1640 (200 μl) simultaneously. In other experiments, ritonavir or RPMI-1640 was also administered intraperitoneally into mice as the same doses stated above, beginning on day 4 for 18 days.

In situ *hybridization*

EBERs were detected by *in situ* hybridization using fluorescein isothiocyanate (FITC)-conjugated EBER PNA (peptide nucleic acid)-probe (DAKO). Briefly, formalin-fixed, paraffin-embedded tissue sections of tumor and various organs were deparaffinized and hydrated in xylenes and graded alcohol series, then rinsed for 5 min in PBS. Deparaffinized samples were incubated with 10 ng/μl of proteinase K for 20 min at 37°C followed by washing, and then incubated with 0.3% methanol for 30 min at room temperature. After washing in PBS, the sections were hybridized with FITC-conjugated EBER-PNA probe in the hybridization solution for 90 min at 56°C. The slides were washed twice in 0.2 × SSC for 20 min at 56°C, and incubated with anti-FITC monoclonal antibody (DAKO) for 45 min at 37°C. Followed by washing, the slides were incubated with horse-radish peroxidase-conjugated polymer reagent (Envision, DAKO) for 30 min at room temperature. Positive staining was visualized after incubation of these samples with a mixture of 0.05% 3.3′-diaminobenzidine tetrahydrochloride in 50 mM Tris-HCl buffer pH7.6 and 0.01% hydrogen peroxide for 5 min. The samples were counterstained with hematoxlin for 2 min, hydrated completely, cleaned in xylene and then mounted. The samples were visualized and photographed under light microscopy (BX41 and DP70; Olympus, Tokyo, Japan).

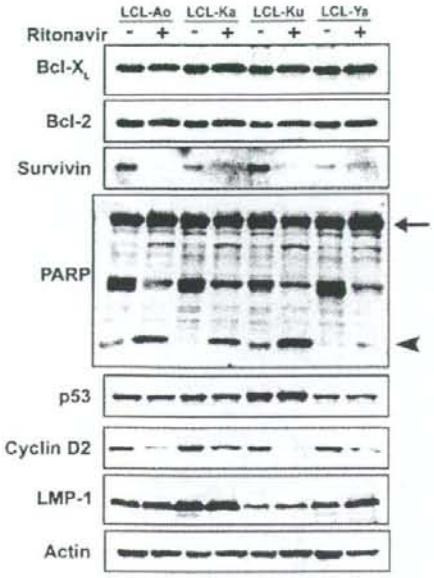

FIGURE 2 – Ritonavir inhibits expression of apoptosis- and cell cycle-associated proteins. EBV-immortalized B-cell lines were cultured with (+) or without (−) ritonavir (40 μM) for 24 hr. Cells were harvested and subjected to Western blot analysis. The polyvinylidene fluoride membrane was sequentially probed with indicated antibodies. Arrow indicates full-length PARP (116 kDa) and arrow head indicates cleaved form of PARP (25 kDa). Essentially the same results were obtained in 3 experiments and representative data are shown.

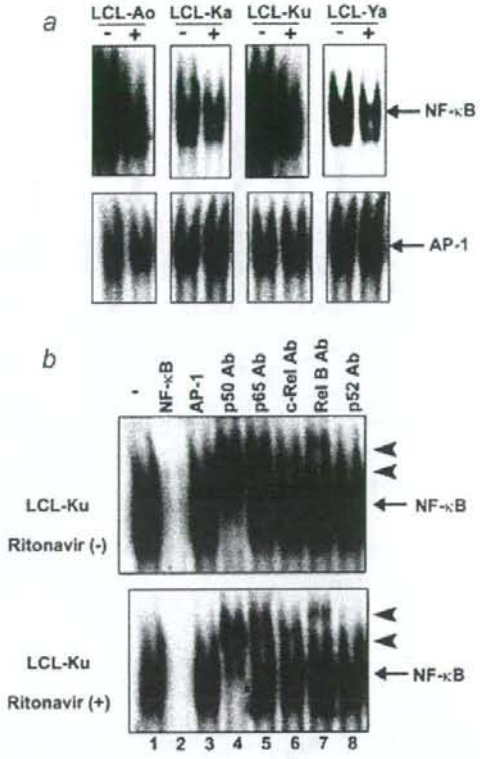

FIGURE 3 – Ritonavir inhibits constitutive NF-κB activation. (*a*) EBV-immortalized B-cell lines were cultured with (+) or without (−) ritonavir (40 μM) for 24 hr and assessed for NF-κB and AP-1-DNA binding activity. (*b*) Cold competition using 100-fold excess of unlabeled NF-κB oligonucleotide, or AP-1 oligonucleotide (lanes 2–3) demonstrated the specificity of the protein/DNA binding complexes. Specificity of NF-κB binding was also determined by using antibodies to the NF-κB components p50, p65, c-Rel, RelB and p52, resulting in supershift (lanes 4–8). Arrows indicate specific complexes of NF-κB with wild type NF-κB oligonucleotide. Arrow heads indicate supershift. Essentially the same results were obtained in 3 experiments and representative data are shown.

Results

Ritonavir induces cell-cycle arrest and apoptosis of LCLs

Ritonavir was examined for its effect on cell-cycle distribution of EBV-immortalized LCLs (Fig. 1*a*). Ritonavir effectively inhibited cell-cycle progression, as evidenced by increased proportion of the cells in G_1 phase of LCL-Ao, LCL-Ka, LCL-Ku and LCL-Ya (LCL-Ao: from 60.1% to 67.1%; LCL-Ka: from 61.2% to 69.9%; LCL-Ku: from 52.6% to 57.3%; and LCL-Ya: from 67.4% to 72.1%). These results indicated that ritonavir induced cell-cycle arrest at G_1-phase. The weak accumulation of cells in G_1 phase by ritonavir suggests that it might rather be an apoptosis inducer than a cell growth inhibitor.

Furthermore, we evaluated the effect of ritonavir on the cell viability of LCLs and PBMCs from healthy individuals (Fig. 1*d*). Ritonavir effectively reduced the survival of LCLs (LCL-Ao, LCL-Ka and LCL-Ku) as measured by WST-8 on the third day of culture in a dose-dependent manner. In contrast, ritonavir hardly affected the survival of PBMCs from healthy volunteers.

The effect of ritonavir on apoptosis was examined by the Annexin-V and PI method. Annexin-V binds to the cells that express phosphatidylserine on the outer layer of the cell membrane, a characteristic feature of cells entering apoptosis. Early apoptotic cells were stained with Annexin V but not with PI. Late apoptotic and necrotic cells were stained with both fluorescent. Ritonavir induced increased proportion of cells positive for Annexin-V and negative for PI in all cell lines (LCL-Ao: from 14.8% to 62.3%; LCL-Ka: from 13.8% to 37.8%; LCL-Ku: from 9.9% to 37.9% and LCL-Ya: from 10.1% to 66.9%) (Fig. 1*b*). Ritonavir also induced dose-dependent increasing of Annexin-V positive and PI negative cells in LCL-Ku cells (Fig. 1*c*), indicating increasing apoptosis of ritonavir-treated cells.

Ritonavir down-regulates the expression of the cell-cycle- and apoptosis-associated genes

The antiproliferative and proapoptotic effects of ritonavir were explored by examining the levels of intracellular regulators of cell-cycle and apoptosis after exposure to ritonavir (Fig. 2). Ritonavir down-regulated the levels of survivin and cyclin D2 in EBV-immortalized B-cell lines. We also observed increased cleavage of PARP in these cells. However, ritonavir did not modulate the other regulators of cell-cycle and apoptosis such as Bcl-X_L, Bcl-2 and p53. Ritonavir had no effect on the expression of viral proteins such as LMP-1, suggesting that ritonavir may induce cell-cycle arrest and apoptosis by down-regulating the levels of survivin and cyclin D2 without reducing the virus levels in the cells.

Ritonavir suppresses constitutive NF-κB expressed by EBV-transformed LCLs

To examine the effect of ritonavir on NF-κB DNA binding, EMSA was performed. EBV-immortalized B-cell lines were incubated with or without 40 μM ritonavir for 24 h, and nuclear extracts were prepared and examined for NF-κB by EMSA.